Pergamon

Int. J. Solids Structures Vol. 35, Nos. 3–4, pp. 219–237, 1998

0020-7683/98 $19.00 + .00

PII: S0020-7683(97)00064-4

OPTIMAL TOPOLOGY DESIGN USING A GLOBAL SELF-ORGANISATIONAL APPROACH

W. M. PAYTEN†, B. BEN-NISSAN‡ and D. J. MERCER†

† Australian Nuclear Science and Technology Organisation, (ANSTO), Materials Division, Private Mail Bag 1, Menai, NSW, 2234, Australia

‡ University of Technology Sydney, Dept of Materials Science, P.O. Box 123 Broadway, NSW, 2007 Australia

(*Received* 15 *October* 1996; *in revised form* 22 *January* 1997)

Abstract—A method based on a self-organisational approach has been developed, where a local state operator defines the state of each finite element at each iteration. The algorithm is based on the principle of local adaptation with global feedback in the form of a derivative equation based on von Mises stresses that allows the local remodelling function to vary at each time step. The state operator has the form of a nonlinear differential equation solved iteratively based on the material density and strain energy density within each element. A constraint equation is formulated based on a maximum deviatoric strain energy criteria, with the objective to minimise the mass of the design domain subject to the above constraint. A number of examples are presented to demonstrate the use of this approach. © 1997 Elsevier Science Ltd.

INTRODUCTION

The class of problems where the definition of the shape forms part of the design problem is known as topology or layout optimisation. These problems are difficult to solve numerically due to the large number of design variables and the large number of equality and inequality constraints. This results in a problem that is ill-posed, with a design universe that can be non-convex in its solution space. The homogenisation method (Strang and Kohn, 1986; Bendsoe and Kikuchi, 1988) solved this problem by relaxation of the object function by introducing a microstructure into the design space.

Recently a number of other techniques have been proposed that simplify the solution to the optimisation problem. These include the evolutionary technique of Stevens and Xie (1993), the linear programming technique of Yang and Chuang (1994), the simulated biological approaches of Mattheck and Burkhard (1990) and Mattheck *et al.* (1993) and the sensitivity approach of Atrek (1989). In this paper an optimisation process is presented that has, as its basis, an algorithm originally developed for predicting anatomical density distributions in natural human bone, (Cowin and Hegedus; 1976, Huiskes *et al.*, 1987; Carter 1987; Carter *et al.*, 1987; Weinans *et al.*, 1993). In its original form as a bone adaptation algorithm, the method was also used by Reiter *et al.* (1993) to improve the design of a composite structure. Only local optimality criteria can be handled and thus the method is limited to problems where global constraints were neglected.

ADAPTIVE ELASTICITY

The theory of adaptive elasticity as it pertains to bone remodelling was originally proposed by Cowin and Hegedus (1976). Their model is based on the principle that the adaptation of living bone is a spatially localised event where a relationship exists between stress, strain and the modification of bone density. They assumed that the rate of adaptation is couples to the difference between the homeostatic strain and the actual strain. The greater this difference, the larger the driving force for adaptive activity. Huiskes *et al.* (1987) extended this approach by setting the bone remodelling rate, proportional to the difference between the homeostatic or reference strain energy density (U_s), and the new strain energy density (U_f). The driving energy will then equal the difference, U_r

$$U_r = U_f - U_s. \tag{1}$$

For an arbitrary solid the total strain energy U is given by the volume integral;

$$U = \int \check{U}\, dv, \tag{2}$$

where $\check{U}$ is the strain energy per unit volume or strain energy density and

$$\check{U} = \tfrac{1}{2}\varepsilon_{ij}\sigma_{ij} \tag{3}$$

where σ_{ij} is the local stress tensor and ε_{ij} is the strain tensor. The strain energy density can also be related to the elasticity tensor E, Poisson's ratio v and shear tensors τ_{ij} by the following;

$$U = \frac{1}{2E}[(\sigma_x^2+\sigma_y^2+\sigma_z^2) - 2v(\sigma_x\sigma_y+\sigma_x\sigma_z+\sigma_z\sigma_y) + 2(1+v)(\tau_{xy}^2+\tau_{xz}^2+\tau_{zy}^2)]. \tag{4}$$

The rate of change of bone density ρ can be described as an objective function which depends upon the strain energy density (stimulus) at a specific location and is directly related to the localised stress (Huiskes *et al.*, 1987);

$$\frac{d\rho}{dt} = F(\sigma, \varepsilon, \rho), \quad 0 < \rho \leqslant \rho_{cb}. \tag{5}$$

The constraints specified in eqn 5 relate to the bone densities: the density of the bone cannot decrease below zero (total reabsorption) or above the density of fully mineralised cortical bone ρ_{cb}. The above system is in equilibrium when the objective function F reaches zero. Equation 5 can be expressed using the following relationship (Huiskes *et al.*, 1987) where the bone stimulus value can be approximated as U/ρ which represents the strain energy per unit of bone mass;

$$\frac{d\rho}{dt} = B\left(\frac{U}{\rho} - k\right) 0 < \rho \leqslant \rho_{cb}. \tag{6}$$

Here, k represents the stimulus objective of the natural bone and B is an adjustment multiplier. Knowing that the strain energy density is related to the elasticity tensor, then the strain energy density changes by modifying the material density.

Finally a relationship is required between density and the elasticity tensor, shown experimentally (for bone) to be approximated by the following power law relationship, Carter and Hayes (1977);

$$E = A\rho^{\gamma}, \tag{7}$$

where $A = 3790$ and $\gamma = 3$.

INSTABILITIES IN THE DISCRETE RATE EQUATION

Although the adaptation rate algorithm is based on a simple equation, recent research has demonstrated instabilities associated with the use of the finite element iterative version of this equation. Weinans *et al.* (1992) showed that a standard finite element post processor graphics program obscured artifacts associated with the algorithm. Using nodal interpolation, a smearing of adjacent densities occurs (which is standard practice in obtaining a smoothed contour plot). In this form the results appear to simulate the actual density distribution in an anatomical model of the femur, with the density contours displaying a

smooth continuous distribution. If the same model is viewed again without nodal interpolation, then a discrete structure is evident along with checker-boarding of the elements. It has been suggested that the resulting structure displays an appearance similar to the network type pattern of the internal bone structure (trabecular bone) which has been hypothesized as showing self-optimised characteristics (Weinans *et al.*, 1992). Closer inspection shows the elements converge to the constraint boundaries of the solution, with each element reaching either full density or disappearing. The iterative solution bypasses the continuous converged density solution within the first few iterations due to the existence of an unstable saddle point. According to Weinans *et al.* (1992), the end solution reached, although showing convergence (i.e., there is no change in structure or mass), is both discontinuous in nature and incorrect in terms of satisfying the objective function. The final solution is unable to satisfy the objective function $U/\rho = k$ such that the rate of change of density $\mathrm{d}\rho/\mathrm{d}t = 0$. This leads to a solution where element stimulus levels are scattered both above and below the set stimulus value k. Weinans *et al.* (1992) also showed using a two element model that the optimisation process results in a chaotic solution, yet paradoxically the final solution of a many element model results in a distinctly non-chaotic structure.

This phenomena has been studied in greater detail (Cowin *et al.*, 1992, 1993), showing that the continuous differential equation predicts smooth, monotonic and non-chaotic behaviour. The chaotic behaviour is a result of the discrete-time computational process and the nonlinear behaviour of the elasticity tensor, density relationship. Cowin *et al.* (1992, 1993) also showed that the discrete time algorithm can be characterised by a logistic one-dimensional map that arises quite commonly in population biology (May, 1976)

$$x_{t+1} = \lambda x_t(1 - x_t), \tag{8}$$

where t is the discrete time, x_{t+1} is the size of a population at $t+1$ and is related to the size x_t of the population in the preceding generation at time t. This equation assumes that the species at any time is self-interacting in an unchanging environment typified by the control parameter λ. The result is an algorithm characterised by Feigenbaum period doubling cascades that lead to chaos, with the control parameter λ determining the onset of period doubling.

In a similar fashion, the scaled density exponent, γ in eqn 7, also controls the onset of instabilities, which occur for values of γ greater than 1, (Cowin *et al.*, 1993). In a further appraisal Harrigan and Hamilton, (1992a, 1992b, 1993, 1994a, 1994b) showed that the objective function is in fact a combination of two indicator functions detailing the global optimisation characteristics of eqn 6. They showed that density taken to a power as a state variable, results in a process of optimisation, of both the weighted sum of the strain energy in the structure and the total mass of the structure. Certain conditions are necessary for this to be ensured.

It should be emphasised that these methods of predicting anatomical bone densities pose many questions in relation to their applicability, as they are not related in any mechanistic way to the biology underlying the development of animal or human bones. Many of the methods developed result in steady state solutions that look like bone from an engineering point of view but the methods in general rely on using mechanisms and pathways completely unrelated to real biology. This is, of course, irrelevant in terms of engineering topology optimisation.

OPTIMISATION PROBLEM

Traditional optimisation using mathematical programming techniques is normally formulated as follows: Find the set of design variables $\mathbf{P} = \{\rho_1, \rho_2, \rho_3, \ldots, \rho_n\}$ that will:

$$\begin{aligned} &\text{minimize} \quad F(\mathbf{P}) \\ &\text{subject to} \quad h(\mathbf{P}) \leqslant \sigma_{lim}, \end{aligned}$$

and the side constraints: $\rho_i^l \leqslant \rho_i \leqslant \rho_i^u$, $i = 1, n$, where $F(P)$ is the objective function and $h(P)$ is an inequality constraint, based in this case on stress and where P is the vector of the design variables and ρ^l and ρ^u are the lower and upper bounds on the 'n' design variables, respectively. The objective of the topology design can be formulated as a relationship between the compliance and the potential energy, with the objective to minimize the compliance which is equivalent to maximizing the stiffness. Further to this we also wish to minimise the mass of the design subject to the inequality and side constraints imposed. This type of nonlinear programming problem can be solved using homogenisation techniques with a suitable mathematical programming technique such as gradient descent methods, Lagrange multiplier etc, if the mass or volume of the desired structure is specified as a constraint. Leaving the objective as maximising the stiffness of the structure using the available constraint volume.

PROGRAM "SELF-OPT"

The goal of this paper was to develop an algorithm based on the unusual properties of eqn 6 without resorting to the more traditional approach detailed above. Thus the algorithm must be able to achieve the development of a single density, minimum volume shape, without overstressed areas, (Payten *et al.*, 1995, Payten, 1996). An important consideration is that any alteration to eqn 7 must be obtained without destroying its self-organisational characteristics. A suitable algorithm can be found by linking the local reference stimulus 'k' to a global feed-back stress parameter, based on the maximum von Mises stress at each iteration. The reference stimulus can then be adjusted by both the local and global situation. This ensures that no elements exceed the maximum stress limit and allows minimisation of the objective based on a self-organisational approach. The locally unstable nature of the original algorithm (eqn 6) is used to ensure that segregation to a real single density structure is achieved.

The bone adaptation equation is modified by changing 'k' the objective stimulus to U_{lim}/ρ. This recasts the problem in terms of a limiting criterion U_{lim}. In this case U_{lim} represents a von Mises stress criterion, posing the problem on a more conventional engineering frame-work. The set stress level must be translated into a strain energy density, as the optimisation will be performed in response to the deviatoric component of the strain energy density U_s. If Y equals the limiting stress, then the energy criterion in terms of strain energy can be approximated using the following criterion;

$$U_{lim} = \left(\frac{1+\nu}{6E}\right) 2Y^2. \tag{9}$$

To incorporate this into the bone adaptation equation, 'k' is first modified by separating the volumetric and deviatoric parts of the strain energy and substituting the limiting strain energy (eqn 9) for the deviatoric component of the stimulus. It is assumed that the volumetric component of the strain energy does not contribute to the shear energy of an isotropic material and hence as we wish to optimise based on the von Mises stress this component is subtracted. The equation in this form behaves similar to the original algorithm, any solution will overshoot the constraint stress, leading to a higher final stress. In order to obtain a solution that does not exceed the solution constraints (von Mises stress), adjustment of the algorithm is required at each time step based on the globally recovered maximum stress. This is achieved by dividing the strain energy component by a suitable global parameter that based on the global maximum von Mises stress. This essentially gives a global feedback to the local equation and has the effect of ensuring that $U_i < U_{lim}$ is satisfied for all elements. For example, if during the solution phase the situation $U_i > U_{lim}$ occurs (meaning that some elements in the modelling domain exceed the stress), then the stimulus U_{lim}/ρ must be adjusted to a smaller value in order to satisfy the global stress constraint. The local stimulus is thus linked to the global solution via the adjustment parameter. Two parameters are introduced to enable local/global linking, ψ and σ_{lim}. The

value σ_{lim} describes the maximum permissible stress in the final shape and is the true global limit. The magnitude of the adjustment parameter, ψ is not known a-priori and relates to the proximity of the system to the prescribed limit stress. Assuming the global stress condition is achieved, then no element will exceed σ_{lim}. The global differential in terms of von Mises stress is stated as;

$$\Delta\psi = \sigma_{vm} - \sigma_{lim}, \tag{10}$$

and the discrete form of eqn 10 is;

$$\psi_{t+1} = \psi_t + \tau(\sigma_{vm} - \sigma_{lim}), \tag{11}$$

where τ is a relaxation parameter and σ_{vm} is the maximum global von Mises stress recovered from the static analysis at each time step. Substituting the discrete expressions for ψ and σ into the adaptation eqn (6) gives

$$\frac{d\rho}{dt} = B\left(\frac{U_i}{\rho_i} - \left[\frac{U_{lim}/(\psi_t + \tau(\sigma_{vm} - \sigma_{lim}))}{\rho_s} + \frac{U_v}{\rho_s}\right]\right) \tag{12}$$

where U_i is the total strain energy in the ith element, U_v is the volumetric strain energy in the ith element, ρ_i is the density in the ith element and ρ_s is the upper bound density. The equation still applies at a local level, element by element. The iterative solution of eqn 12 is still highly unstable in this form in terms of satisfying the global stress constraints. To prevent the problem of an increasing global parameter ψ (when σ_{vm} is decreasing, but higher than σ_{lim}), it is necessary to include the following constraints and conditions defined using a simplified control algorithm;

$$\Delta\sigma = \sigma_{vm}^{t} - \sigma_{vm}^{t-1}, \tag{13}$$

and

$$\psi_{t+1} = \begin{cases} \psi_t + \Delta\psi, & \text{if } \Delta\psi > 0 \wedge \Delta\sigma > 0, \\ \psi_t, & \text{if } \Delta\psi > 0 \wedge \Delta\sigma < 0, \\ \psi_t + \Delta\psi, & \text{if } \Delta\psi < 0 \wedge \Delta\sigma < 0, \\ \psi_t, & \text{if } \Delta\psi < 0 \wedge \Delta\sigma > 0, \end{cases} \tag{14}$$

where σ_{vm}^{t} and σ_{m}^{t-l} are the global maximum von Mises stress in the current and preceding time steps, respectively. The elasticity tensor E of each element at each iteration can then be updated and rewritten to the NISAII file for the next static analysis. This is accomplished by relating E to the density taken to a power γ;

$$E = E_o[\rho + d\rho]^{\gamma}. \tag{15}$$

Solution convergence can be monitored by the following criterion;

$$\phi = \frac{1}{m}\sum_{i=1}\left|\frac{U}{\rho} - \frac{U_{lim}/(\psi_t + \tau(\sigma_{vm} - \sigma_{lim}))}{\rho_s}\right|. \tag{16}$$

In addition, the total mass of the structure is calculated at the end of each step;

$$M = \sum_{i=1} (V^i \rho^i). \tag{17}$$

The ability to predict optimal structures can be demonstrated by applying this new algorithm to engineering problems and comparing the results with those obtained by Suzuki and Kikuchi (1991), Mlejnek and Schirrmacher (1993), Jog *et al.* (1994), Baumgartner *et al.* (1992), Atrek (1989) and Steven and Xie (1993). These methods represent a range of techniques from the Homogenisation technique through to the "soft kill" approach.

RESULTS

A number of cases are examined initially by comparing with simple analytically determinable shapes and then by comparing with geometries analysed via other methods.

Case 1 : *tension bar*

This case models a simple tension bar. A square domain with an arbitrary size of 5 units along each side and 1 unit thick is modelled. The displacements along a 1 unit wide length located at the centre of the left hand edge are fixed at zero and a force of 250 units is applied to the same length on the opposite edge. E_o is 421, a density of 7.8 g/cm^3 is used with γ equal to 3, resulting in a full density structure with E equal to 200 GPa. The algorithm is integrated using a time step $\Delta t = 100$ and a relaxation parameter $\tau = 0.5$. The objective function is set to a shear strain energy equivalent to 240 MPa. The solution for this problem should approximate a design with a constant stress of 250 units along the entire bar with a thickness of 1 unit incorporating a width of 8 elements.

Comparing the original bone adaptation algorithm with the modified algorithm demonstrates the unstable nature of the original algorithm. Figures 1 and 2 show the corresponding converged density distributions. The resulting shape for both algorithms is a tension beam, showing that in this case both methods lead to the design of an optimal shape. However the bone adaptation solution has a smaller thickness leading to higher stresses. The bone adaptation solution obtains a von Mises stress of 374 MPa, exceeding the stress criteria of 250 MPa. The model has a corresponding thickness of 0.75 units, while the modified algorithm produces a structure stressed at the set constraint of 250 MPa and is correspondingly 1 unit thick. For this case both algorithms lead to almost complete segregation of densities into either reabsorbed or full density elements. Although the SELF-OPT algorithm incorporates a global stability criteria, the self-organisational nature of the original function appears to be intact. This is not surprising since the modification adjusts only the stimulus and does not change the function or provide stability to the original algorithm. This result compares favourably with advanced layout theories and the SKO method. A similar case analysed by Mlejnek and Schirrmacher (1993) also results in the same tension beam as produced here.

Case 2 : *two bar frames*

This example considers a two-bar frame and corresponds to problems analysed by Suzuki and Kikuchi (1991), and Steven and Xie (1993). As described by Steven and Xie (1993), "for fixed values of the applied load F and the horizontal length L, the optimal height is obtained as $H = 2L$, if this structure is assumed to be a truss". The model here incorporates the same principles as the previous authors. A rectangular domain larger than the size $L \times 2 \times L$ is used. The mesh incorporates 25×60 isoparametric 4 node quadrilateral elements. As used by Steven and Xie (1993) the Young's modulus is 100 GPa with a Poisson's ratio of 0.3. The time scheme and relaxation parameter are the same as in case 1. As the adaptation involves a change in the density term, the maximum density is arbitrarily set to 5, γ is set to 3 so that the constant E_o equals 800. A stress criterion must be used and is set arbitrary to 250 MPa.

This example accreted to a two bar frame as shown in Fig. 3. The analytical solution to a perfect two-bar is given by $H = 2 \times L$, and both Suzuki and Kikuchi (1992) using the homogenization method and Steven and Xie (1993) using the evolutionary rate method

Fig. 1.

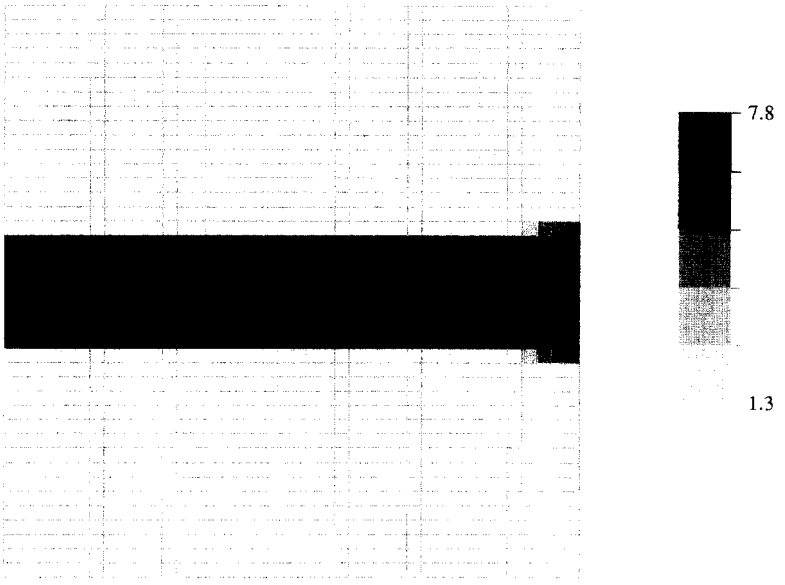

Fig. 2.

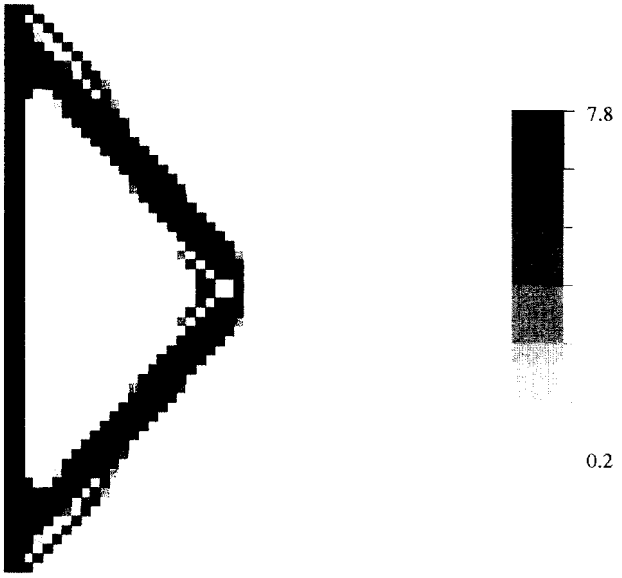

Fig. 3.

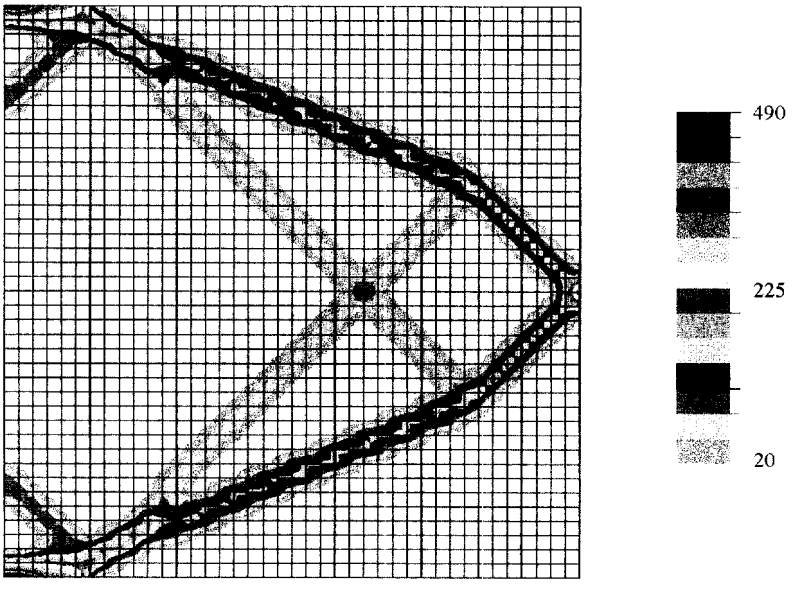

Fig. 4.

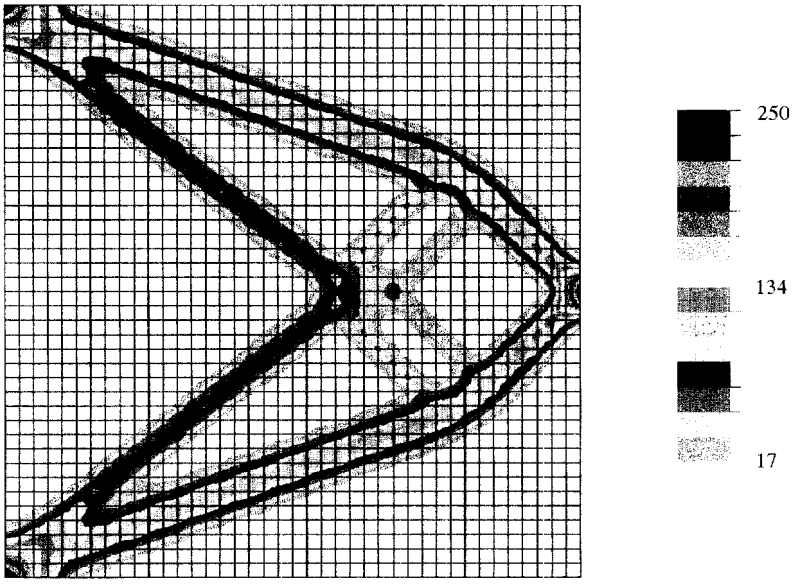

Fig. 5.

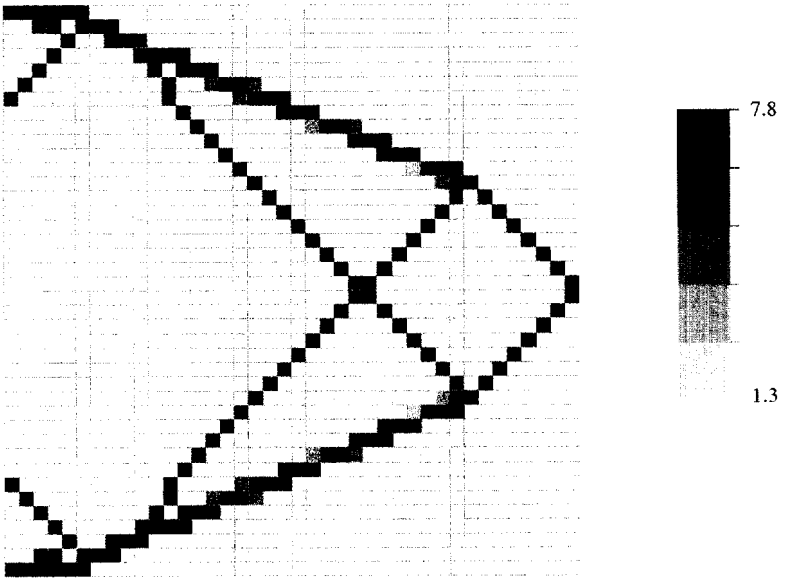

Fig. 6.

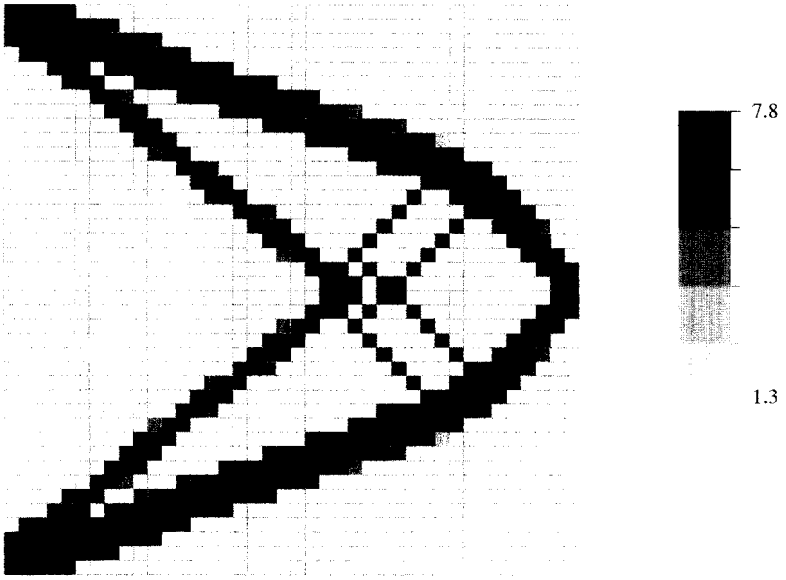

Fig. 7.

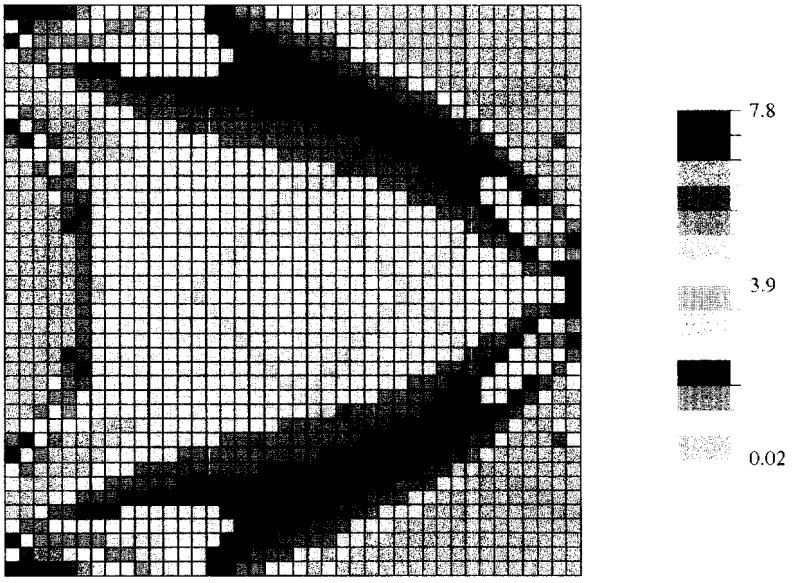

Fig. 8.

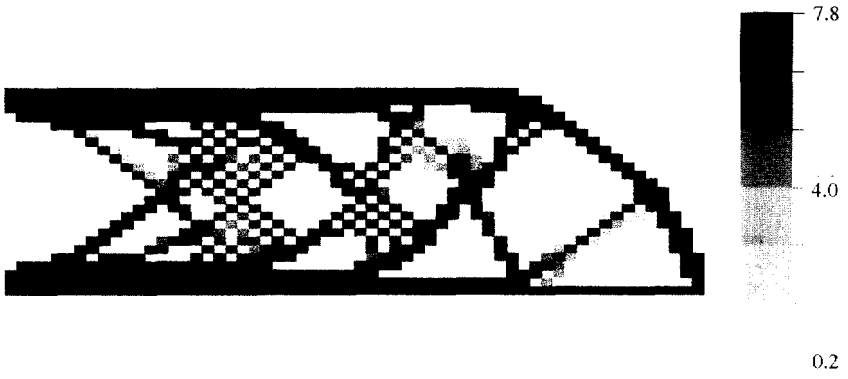

Fig. 11.

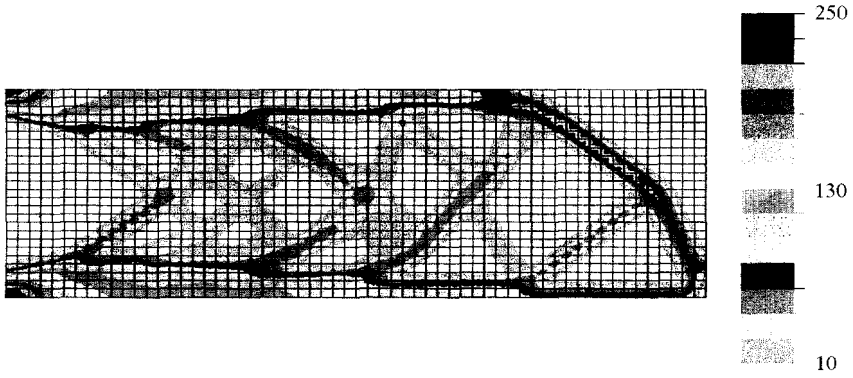

Fig. 12.

Fig. 13.

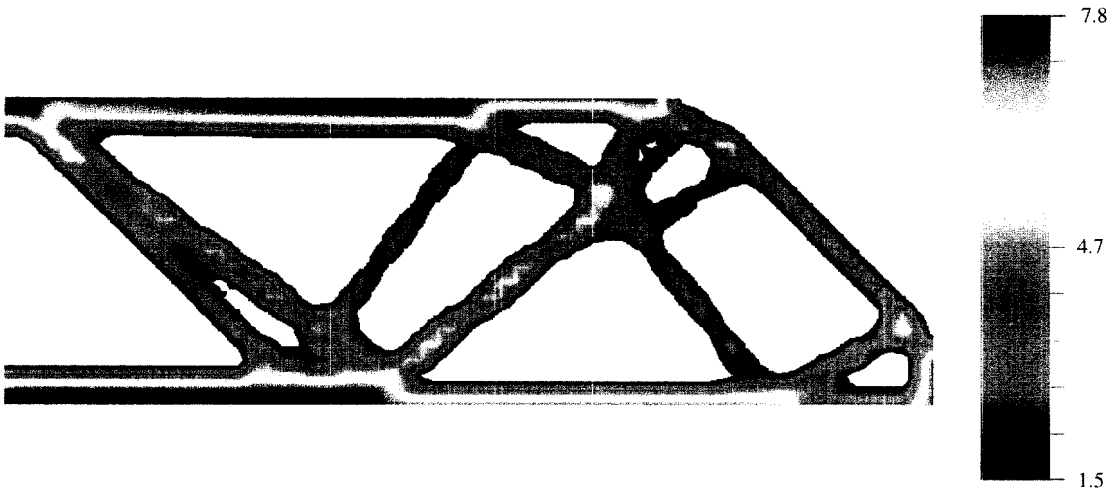

Fig. 14.

Fig. 15.

predicted this result. Using SELF-OPT the thickest truss conformed to the $H = 2L$ ratio, however, two smaller trusses outlying the main truss are formed joining the thick truss to the top and bottom of the spatial domain. This smaller truss developed early in the adaption process, due to initial strain energy density that existed in the full beam at the ends. (Note: that the first two layers of elements along the left hand edge are frozen and do not take part in the adaption process.)

Case 3: *square cantilever*

A square cantilever of edges 5 units in length with a displacement fixed along one edge and a single vertical midpoint load on the opposing side of 50 units was modelled. The same properties and time stepping scheme were used as in case 1. The mesh was discretized into 40×40, 1600 4 node plain stress elements. Noting that the initial maximum stress for the design domain is 193 MPa, the objective function was set equal to 250 MPa, thus allowing the cantilever an increase of 57 MPa during the adaption process. Figures 4 and 5 show the von Mises stress solution for the bone adaptation and local/global algorithms.

As in the tension bar case, the original algorithm shows areas with stresses up to 490 MPa (Fig. 4), while the modified SELF-OPT solution achieves the constraint stress of 250 MPa, (Fig. 5). Ignoring the mass difference and focusing only on the topology, shows that the two algorithms give similar features. Both form the main two outer truss system. However a number of intermediate shear trusses are also formed allowing the main truss to bend where the middle truss intersect it. Figures 6 and 7 detail the corresponding final density distribution for the two algorithms.

The density distributions in Figs 6 and 7 correspond to the stress patterns in Figs 4 and 5, with the SELF-OPT algorithm containing significantly more mass and consequently a lower stress, than the original bone adaptation solution. The SELF-OPT structure shows almost complete discretization to either elements or elements at full density, in this case $7.8/\text{cm}^3$. Out of a total of 401 remaining elements, 66 elements, ($\sim 16\%$) were below full density. However, the majority of these elements had a density greater than $4.0\ \text{g/cm}^3$. The overall mass decrease was 75% taking the stress from 193 to 250 MPa. If the situation $\gamma < 1$ is modelled then the result should be a continuous density distribution as shown in Fig. 8.

The final converged shape shows the initial development of the two main trusses with a lower density internal area and areas of reabsorption on the top and bottom right hand end. The various algorithms and parameter values γ are compared for the mass reduction of the bone adaptation algorithm, the local/global algorithm plus the stable solution when $\gamma < 1$ (Fig. 9).

The behaviour of the local/global algorithm during the solution phase does not display monotonic convergence for the mass reduction. During the initial phase of the solution, the adaptation rate is primarily driven by the local algorithm. The solution overshoots the continuous density stable solution, lowering the distribution of the mass to the extent that the stresses in the system exceeds the local objective function. In this case some elements in the spatial domain exceed the shear energy density value corresponding to a maximum von Mises stress above 250 MPa. Then the global feedback parameter ψ increases, adjusting the local stimulus to a point where the stress in the model decreases. At this stage the global parameter ψ can be quite large causing the stresses to decrease below the stress criterion of 250 MPa. The global parameter re-adjusts causing a rise in stresses. The dynamic readjustment can take several iterations until the limit stress stabilises at the desired global criterion. At this point although the global stress criterion is satisfied the local objective function is not. Figure 10 shows the convergence solution using the two algorithms and various values of gamma γ.

The curves for the local solution show the difference between the convergence integrated over active elements and convergence integrated over all the elements. In the latter case the strain energy objective function is unsatisfied causing a higher convergence as elements accrete out. This is in contrast to the local/global algorithm where an adjustment of the global stability criteria causes the local stimulus function to change, thus enforcing the limit of the global stress criterion. During the majority of the solution phase the two

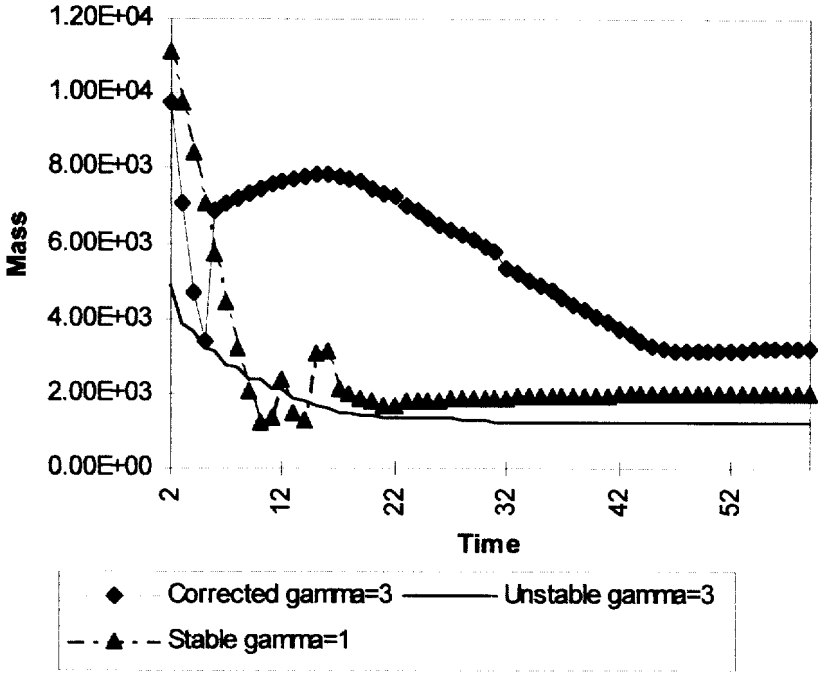
1.20E+04
1.00E+04
8.00E+03
6.00E+03
4.00E+03
2.00E+03
0.00E+00
Mass
2
12
22
32
42
52
Time
Corrected gamma=3
Unstable gamma=3
Stable gamma=1

Fig. 9.

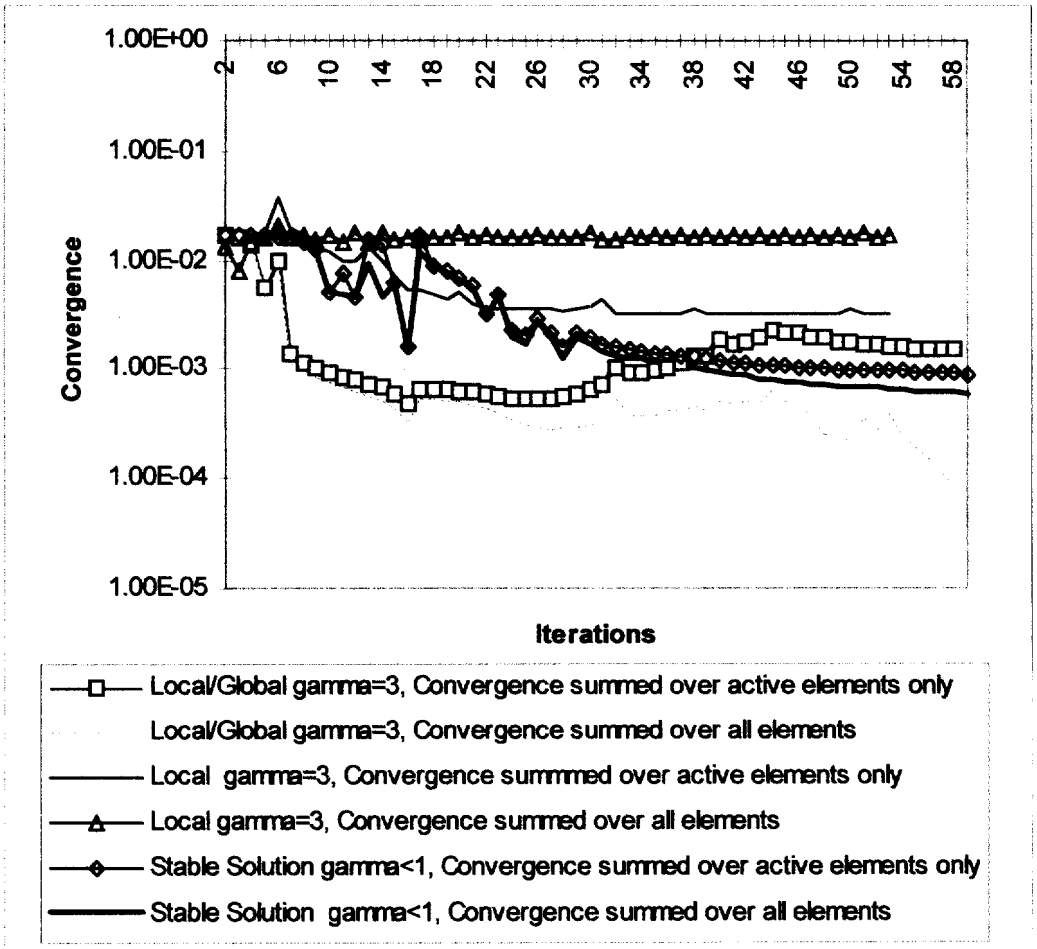
1.00E+00
1.00E-01
1.00E-02
1.00E-03
1.00E-04
1.00E-05
Convergence
2
6
10
14
18
22
26
30
34
38
42
46
50
54
58
Iterations
Local/Global gamma=3, Convergence summed over active elements only
Local/Global gamma=3, Convergence summed over all elements
Local gamma=3, Convergence summmed over active elements only
Local gamma=3, Convergence summed over all elements
Stable Solution gamma<1, Convergence summed over active elements only
Stable Solution gamma<1, Convergence summed over all elements

Fig. 10.

convergences follow closely, deviating late in the solution as the final parts of the structure solidify. This is caused by two factors; firstly the remaining active elements are shielded by the structure now at full density; and secondly the mesh size leaves elements trapped at intermediate densities (they are unable to achieve full density because they cannot reduce in size as the formed truss, in many cases reduces to one element thick). The convergence curve of all elements and the convergence curve using only active elements for the case where $\gamma < 1$ follow each other closely. The final convergence value for this solution is very close to zero. The SELF-OPT algorithm integrated over all elements shows the lowest convergence of any of the solutions. This is due to the forcing nature of the global feedback function. Although the solution stays below 250 MPa (the upper limit), for the local objective function to be fully satisfied, all elements would necessarily show the same stimulus value, representing the equivalent shear energy at 250 MPa divided by the density. This is not the case, the constraint points showing the higher stimulus at 250 MPa whereas the remaining structure shows stimulus levels below this. This is due to the adjustment of the stimulus by the global parameter to keep the solution below the limit, meaning some elements experience a higher than necessary stimulus. The evolution of the structure shows interesting features that can be gleaned from the behaviour of the mass curve. In the initial steps the spatial domain decreases its mass well below the desired density. The algorithm then tends to grow the two main beams first with an area of lower density, 3–4 g/cm^3, occupying the area between the trusses. At this stage the intermediate truss system is then slowly formed from this lower density area. The evolution of these shapes is different from that displayed by Atrek (1988) and Steven and Xie (1993), where the final shape is the result of a process whereby elements are deleted from the design domain, rather than formed. Optimising the cantilever beam from a number of randomly distributed initial density patterns always resulted in very similar structures.

Case 5: *long cantilever*

This problem is also a frequently analysed case. A long cantilever beam, clamped at one end and loaded with a corner vertical force at the opposing end is modelled. Again the modelling parameters are the same with a limit stress of 250 MPa. The design domain consist of a 25×60 4 node isoparametric plain stress elements, 5 units thick. The resultant structure is made of two main beams with a set of cross trusses through the beam's short axis joining the top and bottom beams. The density plot is shown in Fig. 11.

The results are similar, but not identical, to the SKO method (Baumgartner *et al.* (1992) and Mattheck *et al.* (1993)). The algorithm here appears to produce more cross members than the SKO method. The density plot of the SELF-OPT algorithm for this case displayed significant checker boarding of the solution. This problem may be mesh dependent, that is a finer mesh will cause the struts to firm up. A plot of the von Mises stresses show the maximum stress occurring at the centre line obtaining a value of 250 MPa, Fig. 12.

The type of checker boarding seen here was also found by Jog *et al.* (1994), and Suzuki and Kikuchi (1991). The first author suggested using 8 node elements whereas the latter suggested that refining the model would eliminate the 'porous frame' and generate solid frames. Incorporating mid side node elements (parabolic shape function) using SELF-OPT, the checker boarding seen in Fig. 11 is prevented and the structure solidifies out as distinct trusses (Fig. 13). Although 8 node elements produce a "clean" structure it does so slowly compared with 4 node elements.

Case 6: *MBB beam*

This example involves the optimisation of an MBB beam (Messerschmitt-Bolkow-Blohm GmbbH, Munchen, BRD) that is used to carry the floor in an Airbus passenger carrier. This problem has been analysed by various authors (Rasmussen *et al.* (1992) and Olhoff *et al.* (1994)) using the homogenisation, boundary variation method and Steven and Xie (1993) using the evolutionary technique. The problem can be stated as a long centre-loaded beam fixed at one end and free at the opposite end. Due to symmetry only half the beam is modelled. The beam has dimensions of 1200 length, 400 height and 4 mm width.

Based on Steven and Xie (1993), 60*20 quadrilateral elements are used. Young's modulus $E = 200$ GPa, Poisson's ratio $\nu = 0.3$, $\Delta t = 40$ and $\tau = 0.5$, and full density is taken as 7.8 units with a constraint stress of 305 MPa (von Mises stress). The result is shown in Fig. 14.

The various techniques yield somewhat similar topological solutions. Top and bottom beams are formed with various trusses or beams formed between the two main beams. The final design using SELF-OPT results in a structure stressed to the constraint stress of 305 MPa, a deflection of 5.4 mm is generated with a volume reduction of 68% over the initial design. The results show that the SELF-OPT algorithm results in a structure with a large reduction in volume but still retaining excellent stiffness compared with the initial solution.

Case 7: *3-d cantilever*

The final case presented is an extension of the 2-D cantilever beam to 3 dimensions to illustrate the use of the technique in a higher dimension. This model incorporates 8000 elements, and the result as expected shows a similar formation to the 2-D case, with the intermediate trusses angling towards the force constraint as shown in Fig. 15.

CONCLUSIONS

1. A simple algorithm of the type described here appears to have the ability to predict optimal engineering shapes using standard finite element analysis.
2. The shapes produced compare well with other types of engineering layout algorithms with the computational costs involved in the calculation of the local density derivative being minimal.
3. The SELF-OPT algorithm lends itself to the optimisation of structures under imposed stress.
4. Future extensions include multiple load case modelling and eigenvalue optimisation. Work in progress is focused on a more detailed study of stability, control algorithm.

REFERENCES

Atrek, E. (1989) SHAPE: A program for shape optimization of continuum structures. In *Proceedings of the First International Conference on OPTI* 89, Southampton. UK.

Baumgartner, L., Hazheim, L. and Mattheck, C. (1992) SKO (soft kill option): the biological way to find an optimum structure topology. *International Journal of Fatigue* **6**, 387–393.

Bendsoe, M. P. and Kikuchi, N. (1988) Generating optimal topologies in structural design using a homogenization method. *Composite Methods in Applied Mechanical Engineering* **71**, 197–224.

Carter, D. R. and Hayes, W. C. (1977) The behavior of bone as a two-phase porous structure. *Journal of Bone Joint Surgery* **59-A**, 964–962.

Carter, D. R., Fyhrie. D. P. and Whalen, R. T. (1987) Trabecular bone density and loading history: Regulation of connective tissue biology by mechanical energy. *Journal of Biomechanics* **20**, 785–794.

Carter, D. R. (1987) Mechanical loading history and skeletal biology. *Journal of Biomechanics* **20**, 1095–1109.

Cowin, S. C. and Hegedus, D. H. (1976) Bone remodelling I: A theory of adaptive elasticity. *Journal of Elasticity* **6**, 313–326.

Cowin, S. C., Sadegh, A. M. and Luo, G. M. (1992) An evolutionary law for trabecular architecture. *Journal of Biomechanical Engineering* **114**, 129–136.

Cowin, S. C., Arramon, Y. P., Luo, G. M. and Sadegh, A. M. (1993) Chaos in the discrete-time algorithm for bone-density remodelling rate equations. *Journal of Biomechanics* **26**, 1077–1089.

EMRC, Engineering Mechanical Research Corporation, Troy, Michigan, USA :NISAII User Manual.

Harrigan, T. P. and Hamilton, J. J. (1992a) An analytical and numerical study of the stability of bone remodelling theories: Dependence on microstructural stimulus. *Journal of Biomechanics* **25**, 477–488.

Harrigan, T. P. and Hamilton, J. J. (1992b) Optimality conditions for finite element simulation of adaptive bone remodeling. *International Journal of Solids and Structures* **25**(23), 2897–2906.

Harrigan, T. P. and Hamilton, J. J. (1993) Finite element simulation of adaptive bone remodelling: A stability criterion and a time stepping method. *International Journal of Numerical Methods in Engineering* **25**, 837–854.

Harrigan, T. P. and Hamilton, J. J. (1994a) Necessary and sufficient conditions for global stability and uniqueness in finite element simulations of adaptive bone remodeling. *International Journal of Solids and Structures* **31**(1), 97–107.

Harrigan, T. P. and Hamilton, J. J. (1994b) Bone remodeling and structural optimization. *Journal of Biomechanics* **27**, 323–328.

Huiskes, R., Weinans, H., Grootenboer, J., Dalstra, M., Fudala, B. and Slooff, T. J. (1987) Adaptive bone-remodelling theory applied to prosthetic-design analysis. *Journal of Biomechanics* **20**, 1135–1150.

Jog, C. S., Haber, R. B. and Bendsoe, M. P. (1994) Topology design with optimised, self-adaptive materials. *International Journal of Numerical Methods in Engineering* **37**, 1323–1350.

Mattheck, C. and Burkhardt, S. (1990) A new method of structural shape optimization based on biological growth. *International Journal of Fatigue* **12,** 185–190.

Cowin, S. C., Arramon, Y. P., Luo, G. M. and Sadegh, A. M. (1993) Chaos in the discrete-time algorithm for bone-density remodelling rate equations. *Journal of Biomechanics* **26,** 1077–1089.

EMRC, Engineering Mechanical Research Corporation, Troy, Michigan, USA :NISAII User Manual.

Harrigan, T. P. and Hamilton, J. J. (1992a) An analytical and numerical study of the stability of bone remodelling theories: Dependence on microstructural stimulus. *Journal of Biomechanics* **25,** 477–488.

Harrigan, T. P. and Hamilton, J. J (1992b) Optimality conditions for finite element simulation of adaptive bone remodeling. *International Journal of Solids and Structures* **25**(23), 2897–2906.

Harrigan, T. P. and Hamilton, J. J. (1993) Finite element simulation of adaptive bone remodelling: A stability criterion and a time stepping method. *International Journal of Numerical Methods in Engineering* **25,** 837–854.

Harrigan, T. P. and Hamilton, J. J. (1994a) Necessary and sufficient conditions for global stability and uniqueness in finite element simulations of adaptive bone remodeling. *International Journal of Solids and Structures* **31**(1), 97–107.

Harrigan, T. P. and Hamilton, J. J. (1994b) Bone remodeling and structural optimization. *Journal of Biomechanics* **27,** 323–328.

Huiskes, R., Weinans, H., Grootenboer, J., Dalstra, M., Fudala, B. and Sloof, T. J. (1987) Adaptive bone-remodelling theory applied to prosthetic-design analysis. *Journal of Biomechanics* **20,** 1135–1150.

Jog, C. S., Haber, R. B. and Bendose, M. P. (1994) Topology design with optimised, self-adaptive material. *International Journal of Numerical Methods in Engineering* **37,** 1323–1350.

Mattheck, C. and Burkhardt, S. (1990) A new method of structural shape optimization based on biological growth. *International Journal of Fatigue* **12,** 185–190.

Mattheck, C., Baumgartner, L., Kriechbaum, R. and Walther, F. (1993) Computer methods for the understanding of biological optimization mechanisms. *Computational Materials Science* **1,** 302–312.

May, R. (1976) Simple mathematical models with very complicated dynamics. *Nature* **261,** 459–467.

Mlejnek, H. P. and Schirrmacher, R. (1993) An engineer's approach to optimal material distribution and shape finding. *Composite Methods in Applied Mechanical Engineering* **93,** 1–26.

Olhoff, N., Bendsoe, M. P. and Rasmussen, J. (1991) On CAD-integrated structural topology and design optimization. *Composite Methods in Applied Mechanical Engineering* **89,** 259–279.

Payten, W. M., Mercer, D. J. and Ben-Nissan, B. (1995) A non-linear self organisational approach to the solution of optimal structure topology. In *Computational Techniques and Applications*, ed. May, R. World Scientific.

Payten, W. M. (1996) Integrated computer aided design, finite element analysis and bone remodelling of a modular ceramic knee prosthesis. Ph.D. thesis, University of Technology, Sydney, NSW, Australia.

Rasmussen, J. (1990) Collection of examples, CAOS optimization system, 2nd Edition, Special Report No. 1c. Institute of Mechanical Engineering, Aalborg University, Denmark.

Reiter, T. J., Rammerstorfer, F. G. and Bohm, H. J. (1993) Structural design improvement by functional adaptation. In *Structural optimization* 93: Proceedings of the world congress on optimal design of structural systems, ed. J. Herskovits, Rio de Janeiro August 2–6, 1993.

Steven, G. P. and Xie, Y. M. (1993) Evolutionary optimization with FEA. In *Computational mechanics: from concepts to computations*. Proceedings of the second Asian-Pacific Conference on Computational Mechanics, eds S. Valliappan *et al.* Sydney, N.S.W. Australia.

Strang, G. and Kohn, R. V. (1986) Optimal design in elasticity and plasticity. *International Journal of Numerical Methods in Engineering* **22,** 183–188.

Suzuki, K. and Kikuchi, N. (1991) A homogenization method for shape and topology optimization. *Composite Methods in Applied Mechanical Engineering* **93,** 291–318.

Weinans, H., Huiskes, R. and Grootenboer, H. J. (1992) The behaviour of adaptive bone-remodelling simulation models. *Journal of Biomechanics* **25,** 1425–1441.

Weinans, H., Huiskes, R., van Rietbergen, B., Sumner, D. R., Turner, T. M. and Galante, J. O. (1993) Adaptive bone remodelling around bonded noncemented total hip arthroplasty: a comparison between animal experiments and computer simulation. *Journal of Orthopaedic Research* **11,** 500–513.

Yang, R. J., Chuang, C. H. (1994) Optimal topology design using linear programming. *Computers and Structures* **52,** 265–275.